AAPS PharmSciTech, Vol. 12, No. 4, December 2011 (© 2011)
DOI: 10.1208/s12249-011-9695-x

Research Article

Methotrexate-Loaded Chitosan- and Glycolchitosan-Based Nanoparticles: A Promising Strategy for the Administration of the Anticancer Drug to Brain Tumors

Adriana Trapani,[1,4] Nunzio Denora,[1] Giuliano Iacobellis,[2] Johannes Sitterberg,[3] Udo Bakowsky,[3] and Thomas Kissel[3]

Received 24 February 2011; accepted 12 September 2011; published online 27 September 2011

Abstract. Brain tumor treatment employing methotrexate (MTX) is limited by the efflux mechanism of Pg-p on the blood–brain barrier. We aimed to investigate MTX-loaded chitosan or glycol chitosan (GCS) nanoparticles (NPs) in the presence and in the absence of a coating layer of Tween 80 for brain delivery of MTX. The effect of a low Tween 80 concentration was evaluated. MTX NPs were formulated following the ionic gelation technique and size and zeta potential measurements were acquired. Transport across MDCKII-MDR1 monolayer and cytotoxicity studies against C6 glioma cell line were also performed. Cell/particles interaction was visualized by confocal microscopy. The particles were shown to be cytotoxic against C6 cells line and able to overcome MDCKII-MDR1 cell barrier. GCS-based NPs were the most cytotoxic NPs. Confocal observations highlighted the internalization of Tween 80-coated fluorescent NPs more than Tween 80-uncoated NPs. The results suggest that even a low concentration of Tween 80 is sufficient for enhancing the transport of MTX from the NPs across MDCKII-MDR1 cells. The nanocarriers represent a promising strategy for the administration of MTX to brain tumors which merits further investigations under *in vivo* conditions.

KEY WORDS: blood–brain barrier overcoming; confocal microscopy; glycol chitosan and chitosan nanoparticles; P-glycoprotein; Tween 80.

INTRODUCTION

Brain tumors are the most aggressive forms of cancer, and their treatment still presents one of the biggest challenges in oncology. The standard treatment for brain tumors consists of maximal surgical resection, followed by radiotherapy and chemotherapy. Current research efforts are devoted to define the best antineoplastic agent and the optimal delivery system to achieve site-specific chemotherapy (1,2). However, despite continued research and new approaches, the prognosis for patients with malignant brain tumors remains extremely poor. These disappointing results can be related to the inability to deliver therapeutic agents to the central nervous system (CNS) across the blood–brain barrier (BBB). Actually, the BBB is in part compromised at level of brain tumors, where a disrupted and "leaky" BBB occurs. However, the outer rim of the tumor is characterized by a BBB still intact and functional (2). Moreover, it is now well established that a tumor must develop its own vascular network to grow and the neo-vasculature within tumors consists of vessels with increased permeability due to the presence of large endothelial cell gaps compared with normal vessels (3).

Polymeric nanoparticles (NPs) have received increased attention for their ability to deliver anticancer drugs to CNS due to their small size, prolonged circulation time, and sustained drug release profile (4). It is well known that following intravenous administration, polymeric NPs can extravasate into the disorganized and leaky architecture of the brain tumor. This passive targeting of NPs into the brain with disrupted BBB is known as "enhanced permeability and retention (EPR)" effect. Moreover, uptake of NPs can occur at the level of the intact BBB of the outer rim of the tumor through receptor-mediated endocytosis according to Kreuter's research results. In fact, since Kreuter' s first report (5), Tween™ 80 coating layer of hydrophobic NPs was revealed to be indispensable for brain delivery because the surfactant selectively adsorbs apolipoproteins E and B from the blood and these proteins promote receptor-mediated endocytosis of the same particles by the endothelial cells of the BBB. More recently, Gelperina *et al*. (6) also focused on the role of another plasma protein, apolipoprotein A-I, in the interaction with Tween™ 80-coated NPs as a preliminary step to cross the BBB. Tween™ 80-coated NPs investigated were based on hydrophobic polymers such as poly-alkyl-cyanoacrylate (5) and poly(lactide-co-glycolide) (6) as well as the hydrophilic albumin (7).

[1] Department of Pharmaceutical Chemistry, School of Pharmacy, University of Bari, Aldo Moro, Via Orabona, 4, 70125 Bari, Italy.
[2] Department of Chemistry, University of Bari, Aldo Moro, Via Orabona, 4, 70125 Bari, Italy.
[3] Department of Pharmaceutics and Biopharmacy, Philipps-University, Ketzerbach 63, 35032 Marburg, Germany.
[4] To whom correspondence should be addressed. (e-mail: atrapani@farmchim.uniba.it)

In the present study, we aimed to evaluate the *in vitro* performances of Tween™ 80 coated-chitosan-based (CS; Fig. 1a) and glycol chitosan-based (GCS; Fig. 1b) NPs, both loaded with methotrexate (MTX; Fig. 1c) potentially useful for brain tumor treatment. MTX, a competitive inhibitor of dihydrofolate reductase, is widely used in the treatment of malignancies, including childhood acute lymphocytic leukemia, osteosarcoma, non-Hodgkin's lymphoma and head and neck cancer tumors (8,9). Interestingly, reliable cytocidal concentrations of MTX in the cerebrospinal fluid of the CNS malignancies patients were found to be as low as 1 μmol/l (8). However, integral proteins of ABC family, including P-glycoprotein (P-gp), participate in the development of resistance to antifolates, by impairing the transmembrane transport caused by the loss of functions of the reduced folate receptor (10,11). Consequently, free MTX is found to be pumped off by Pg-p which is widely expressed in brain tissue at the apical side of the BBB (1,2,12)

CS-based nanospheres have previously demonstrated good delivery ability for hydrophilic molecules (13–15) and for hydrophilic anticancer drugs such as doxorubicin into murine brain (16). However, the applications of CS for drug delivery are somewhat limited due to its poor solubility at physiological pH values. Therefore, in this work, we decided to investigate also the role played by GCS-based NPs. GCS, indeed, is a chitosan derivative conjugated with ethylene glycol branches, which is water soluble at neutral/acidic pH values. For cancer therapy, several authors have already demonstrated that GCS-based nanocarriers are promising vehicles for anticancer drug delivery (17–19). It was shown by Soni *et al.* (20) that Tween™ 80-coated-^{99m}Tc-radiolabeled CS NPs demonstrated translocation from blood to brain. However, the amount of Tween™ 80 used by the authors was very high.

In this work, the results of *in vitro* studies concerning preparation, physicochemical characterization, cytotoxicity evaluation, and transport across Madin–Darby canine kidney *mdr1*-transfected cell line (MDCKII-MDR1) (21) of the aforementioned CS (and GCS) NPs are reported.

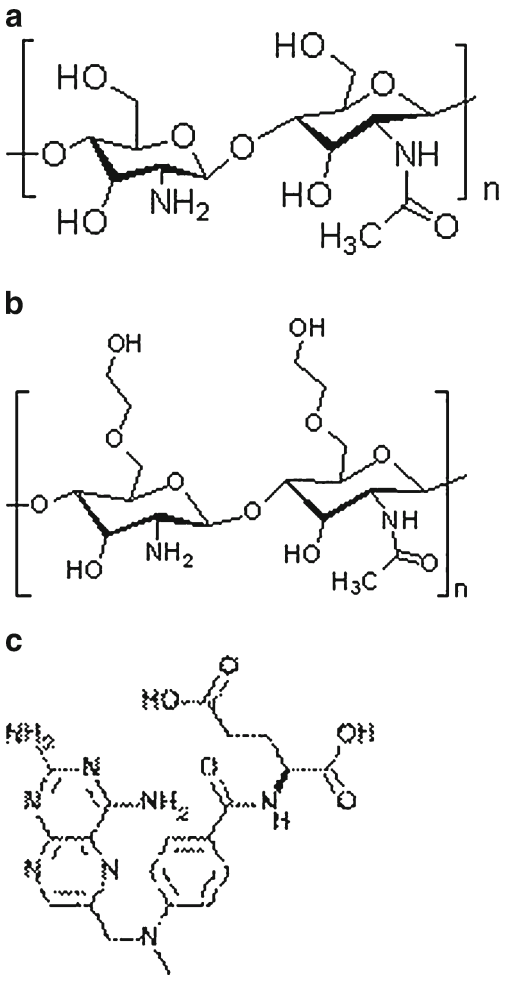

Fig. 1. The chemical structures of chitosan **a**, glycol chitosan **b**, and metothrexate **c**

MATERIALS AND METHODS

Materials

The following chemicals were obtained from commercial sources and used as received. Methotrexate was a gift from Prof. Rosario Pignatello (University of Catania, Italy). Chitosan hydrochloride (UP CL, 113; Mw, 110 kDa; deacetylation degree, 86%; viscosity, 13 mPa×s^{-1} according to manufacturer data sheet) was purchased from Pronova Biopolymer (Norway). Tween™ 80, glycol chitosan (Mw, 68 kDa; from gel permeation chromatography), glycerol, fluorescein-isothiocianate (FITC), fluorescein-dextran 4,000 (FD4), and pentasodium tripolyphospate (TPP) were purchased from Sigma-Aldrich (Milan, Italy). Ultrapure water (Carlo Erba, Italy) was used throughout the study. All other chemicals were reagent grade.

Methods

Preparation of MTX Nanoparticles

CS- or GCS-based nanoparticles were prepared according to a modified procedure of the ionic gelation technique (22).

(a) *Unloaded CS (and GCS) NPs*—unloaded CS NPs were prepared at room temperature by adding under magnetic stirring (VWR, VMS C-4, Milan Italy) 0.65 mL of TPP aqueous solution (0.07%, *w*/*v*) to 0.75 mL of CS (0.2%, *w*/*v*) previously dissolved in acetic acid (1%, *w*/*v*; CS/TPP ratio was 3.3/1.0 (*w*/*w*)). Unloaded GCS NPs were prepared by adding under stirring 0.95 mL of TPP aqueous solution (0.07%, *w*/*v*) to 0.75 mL of GCS (0.2%, *w*/*v*) previously dissolved in acetic acid (1%, *w*/*v*; GCS/TPP ratio was put equal to 2.2/1.0 (*w*/*w*)).

For Tween™ 80-coated CS (GCS) NPs, 150 μL of an aqueous solution of the surfactant (0.01%, *w*/*v*) were previously mixed with the CS solution (or the GCS solution) before the addition of TPP. The final concentration of Tween™ 80 in the NP dispersion was 0.1% (*v*/*v*). Afterwards, NPs were formulated following the procedure mentioned above.

(b) *MTX-loaded CS (and GCS) NPs*—to a TPP aqueous solution (0.07%, *w*/*v*) MTX was added to provide a final concentration of 0.05% (*w*/*v*) of the antitumor drug. CS (GCS) NPs were prepared at room temperature by adding

under stirring 0.65 mL of MTX/TPP aqueous solution of MTX/TPP to 0.75 mL of acetic acid solution of CS (0.2%, *w*/*v*) whereas 0.95 mL of MTX/TPP solution were employed to crosslink 0.75 ml of acetic acid solution of GCS (0.2%, *w*/*v*).

For Tween™ 80-coated NPs, 150 μL of an aqueous solution of the surfactant (0.01%, *w*/*v*) were mixed with the CS phase (or the GCS phase) prior to add MTX. As above, the final concentration of Tween™ 80 in the NP dispersion resulted equal to 0.1% (*v*/*v*).

The resulting NPs obtained as above were isolated by centrifugation (16,000×*g*, 45 min, Eppendorf 5415D, Eppendorf, Germany) and resuspended in ultrapure water by manual shaking.

Physicochemical and Morphological Characterization of Nanoparticles

The mean particle size and the size distribution of freshly prepared particles were determined in double-distilled water by dynamic light scattering using Zetasizer NanoZS (ZEN 3,600, Malvern, Herrenberg, Germany). Samples were measured undiluted at 25°C adjusted to the temperature 2 min prior to the measurement. The autocorrelation functions were analyzed using the DTS v. 5.1 software provided by Malvern. Measurements were done in triplicate with 20 runs each, and the calculated mean values were used. The determination of the ζ-potential was performed using the technique of laser Doppler velocimetry using Zetasizer NanoZS after dilution with KCl 1 mM (pH 7.0) following a procedure already reported (23)

Atomic Force Microscopy

Atomic force microscopy (AFM) was carried out to characterize the morphology of NPs. For AFM visualization, a drop of nanoparticle suspension was diluted in milliQ water (pH 5.5) and dried onto a glass surface. The observations were performed with a JPK NanoWizard (JPK Instruments, Si_3N_4 tips on a cantilever with a length of 125 μm, a resonance frequency of about 220 kHz and a nominal force constant of 36 N/m (NSC16 AlBs, Micromasch, Estonia). To avoid damage of the sample surface, all measurements were conducted in intermittent contact mode. The scan speed was proportional to the scan size with a scan frequency from 0.5 to 1.0 Hz. Images were obtained by displaying amplitude, signal of the cantilever in the trace direction (22).

Chromatographic Analysis

High-performance liquid chromatography (HPLC) analyses of MTX were performed with a Waters (Waters Corp., Milford, MA) Model 600 pump equipped with a Waters 2,996 photodiode array detector (set at the wavelength of 313 nm), a 20 μl injection loop autosampler (Waters 717 plus), and processed by Empower™ Software Build. For analysis, a reversed-phase symmetry (25 cm×4.6 mm; 5 μm particles; Waters) column in conjunction with a precolumn C18 insert was eluted with 60:40 (*v*/*v*) acetonitrile/water in isocratic mode. The flow rate of 0.3 mL/min was maintained, and the column effluent was monitored continuously at 313 nm. Quantification of the compound was carried out by measuring the peak areas in relation to those of standards chromatographed under the same conditions. Standard calibration curves were prepared at 313 nm wavelength using an aqueous solution of TPP (0.07%, *w*/*v*) as solvent and were linear (r^2>0.999) over the range of tested concentrations (2.2×10^{-6}–2.2×10^{-4} M). The retention time of MTX was 5.0 min.

The association efficiency (A.E.) of MTX to the particles was calculated as follows:

$$\%\text{A.E.} = 100 \times (\text{Total MTX} - \text{Free MTX})/\text{Total MTX} \quad (1)$$

The association efficiency values were the average of three batches.

For cell experiments (see below) and taking into account that diazepam (DZ) is a marker of transcellular transport, the HPLC analysis of this drug was carried out using a reversed-phase Varian column (15 cm×4.6 mm; 5 μm particles) in conjunction with a precolumn C18 insert was eluted with 80:20 (*v*/*v*) methanol/water in isocratic mode. The flow rate of 1.0 mL/min was maintained and the column effluent was monitored continuously at 242 nm. The retention time of DZ was 4 min.

In Vitro Release Study

In vitro release tests from MTX-loaded CS (and GCS) NPs in the presence and in the absence of Tween™ 80 was carried out for 72 h in phosphate-buffered saline (PBS; pH 7.4). First, each type of NPs was freshly prepared and then centrifuged in presence of 10 μL of glycerol. For each experiment, in screw-capped test tubes, an amount of particles corresponding to a MTX concentration of about 120 ng/mL was dispersed in 2.5 mL of PBS. The tubes were put in a shaken water bath under mechanical agitation (100 agitation/min) at 37°C. Aliquots of 0.4 mL at scheduled times (0, 0.5, 1, 2, 4, 6, 8, 24, 48, and 72 h) were then withdrawn and replaced with fresh medium of equivalent volume. Each sample was subjected to centrifugation at 16,000×*g* for 45 min. The supernatant was analyzed for the content of MTX by HPLC.

The cumulative release percentage (CR%) of MTX at each time point was calculated using the following equation:

$$\text{CR\%} = \text{amount of MTX in the supernatant}/\text{total amount of MTX in the particles} \times 100 \quad (2)$$

Each experiment was performed in triplicate. Standard deviation of measurements was <5%.

Cell Culture

Madin–Darby canine kidney (MDCKII-MDR1) cells (passages 23–32) were kindly donated by the Netherlands Cancer Institute and grown in Dulbecco's modified Eagle's medium (DMEM) containing glucose (4.5 g/l; Euroclone, Italy) supplemented with 10% fetal bovine serum (Euroclone, Italy) penicillin (100 U/mL), streptomycin (100 μg/mL), and 2 mM L-glutamine.

Rat glioma glial cells (C6; passages 27–30) were grown in Ham's nutrient mixture F-12 medium (Euroclone, Italy) supplemented with 10% fetal bovine serum, penicillin (100 U/mL), streptomycin (100 μg/mL), and 2 mM L-glutamine. Cell cultures were kept at 37°C in an atmosphere of 95% air and 5% CO_2.

Cytotoxicity Studies

In vitro cytotoxicity of control NPs in the presence and in the absence of Tween™ 80 was evaluated using the MTT assay. MDCKII-MDR1 and C6 glioma cells were seeded into 96-well microtiter plates (3,596 Cell Culture Microplate Corning Costar Corp., Germany) at a density of 3×10^4 cells/cm^2. After 24 h, the culture medium was replaced with 100 μL/well of serial dilutions of the samples in complete medium (n of wells/NP concentration=8). MDCKII-MDR1 cells were exposed to unloaded NPs (1.0–0.01 mg/mL) for 3 and 24 h. C6 cells were incubated with unloaded NPs (1.0–0.01 mg/mL) and MTX NPs (0.1–0.001 mg/mL) for 24 h. For both cell lines, sodium dodecyl sulfate was used as positive control at the concentration of 2% (*w*/*v*) in complete cell medium.

After an incubation period of 3 h (or 24 h), the samples were aspirated. Separately, 3-(4,5-dimethyl-thiazol-2-yl)-2,5-diphenyl tetrazolium bromide (MTT; Sigma-Aldrich, Italy) was dissolved in phosphate-buffered saline at 5 mg/mL and 100 μL of the final concentration of 0.5 mg of MTT/mL in FBS-free DMEM were added to each well. After an incubation time of 4 h, the unreacted dye was removed by aspiration and the purple formazan product was dissolved in 100 μL/well dimethyl sulfoxide and quantitated by a plate reader (Victor™ X3, 2,030 Multilabel Reader, PerkinElmer, Italy) at wavelengths of 570 and 690 nm. The relative cell viability (%) related to control wells containing cell culture medium without sample was calculated by (A test/A control)×100. The IC_{50} was defined as the sample concentration inhibiting 50% cell viability.

Transport of MTX and MTX NPs across MDCKII-MDR1 Cell Monolayers

MDCKII-MDR1 cells (passages 23–32) were grown to 70% confluence for 8 days. Cells were seeded at a density of 5×10^4 cells/cm^2 on uncoated polycarbonate Transwell™ filter inserts (3,402 Corning Costar Corp., Germany, 3 μm pore size; area, 1.12 cm^2), and the medium was changed every day. On the day of the experiment, cells were rinsed twice and equilibrated at 37°C for 30 min with the assay medium. The assay medium had the following composition: K_2HPO_4, 0.4 mM; $NaHCO_3$, 25.0 mM; KCl, 3.0 mM; $MgSO_4$, 1.2 mM; $CaCl_2$, 1.4 mM; NaCl, 122.0 mM; and glucose, 10.0 mM. The pH was adjusted to be 7.4, and the osmolarity was 300 mOsm/kg (Micro-Osmometer Automatic Type 13 RS, Hermann Roebling Messtechnik, Berlin, Germany). MTX-loaded NPs in the presence and in the absence of Tween™ 80 were freshly prepared and resuspended in 2 mL of assay medium containing the paracellular marker FD4 (200 μg/mL) and the transcellular marker DZ (75 μM) (24). After the assay medium was aspirated, the cells were apically incubated with 0.5 mL of MTX-loaded NPs suspensions at a particle dose of 0.1 mg/mL for 3 h at 37°C. To evaluate efflux mechanisms, verapamil (VER; 0.1 mM) was added in the assay buffer 5 min prior to the addition of NPs at the apical side. In the control wells (*i.e.*, pure MTX as well as pure FD4 and DZ), the same media without NPs were used. At $t=0$, samples from the apical media were collected to precisely calculate the total amounts of MTX, DZ, and FD4 present in the apical chamber. At fixed times, withdrawals of 0.3 mL from the basolateral compartment were analyzed for MTX permeated. The permeated FD4 was assayed by fluorometric assay (Victor™ X3, 2030 Multilabel Reader, PerkinElmer, Italy, Excitation: 485 nm; Emission 535 nm) whereas DZ was quantitatively determined by means of the HPLC method previously described.

The apparent permeability coefficient P_{app} was calculated using the following equation:

$$P_{app} = dQ/dt(1/A \times 60 \times c_0) \quad (3)$$

where dQ/dt is the permeability rate (in μg/min), namely the amount of MTX permeating the monolayer in time t (in min) obtained from the permeation profiles; A is the diffusion area of the monolayer; c_0 is the initial MTX concentration (in mg/mL).

The enhancement ratio was calculated for each sample as the ratio between the P_{app} obtained in presence of NPs with respect to P_{app} obtained for pure MTX.

During the experiments, the integrity of the monolayers was checked by means of transepithelial electric resistance (TEER) measurements at prefixed times before and after the experiment using a volt ohmmeter (World Precision Instruments, Germany) equipped with Endohm electrodes. The monolayers exhibiting 140–440 Ωcm^2 TEER were used for the experiments.

Preparation of FITC-Labeled CS and GCS

For confocal laser scanning microscopy analysis, CS and GCS were labeled with fluoresceine isothiocyanate (FITC) following reported procedures (25,26) with slight modifications; 80 mg of the polymer were dissolved in 4 mL of 1N HCl, and, thereafter, the pH was adjusted to 6.5 with 3 mL of 1N NaOH. For GCS labeling, 200 mg of the polymer were dissolved in 5 mL of 1N HCl, and thereafter the pH was adjusted to 6.5 with 3 mL of 1N NaOH. 0.4 mL of FITC solution (20 mg/mL in ethanol) were added to the above prepared CS/GCS solutions, the resulting mixtures were stirred at room temperature for 24 h. Then, the mixtures were dialyzed in water using dialysis tubing (SpectraPore® Dialysis MWCO 10,000) for 3 days and freeze dried for at least 48 h. All the preparative steps were carried out under light protection.

To determine the labeling efficiency, the fluorescence intensity of a solution of FITC-polymer dissolved in 0.1 M acetic acid and diluted with phosphate buffer, pH 8.0, until a final concentration of 0.5 μg/mL was reached. Labeling efficiency (%) was calculated as the percent weight of FITC to weight of the FITC-polymer. The fluorometer was calibrated with standard solutions of 1 to 140 ng/mL of FITC prepared by diluting 100 μg/mL methanolic solutions of FITC with phosphate buffer, pH 8.0 (excitation and emission wavelengths of 488 and 525 nm, respectively; slits, 2.5 cm) (27).

Confocal Laser Scanning Microscopy

MDCKII-MDR1 cells (passages 23–32) were grown to 70% confluence for 8 days. Cells were seeded at a density of 5×10^4 cells/cm^2 on 12 wells uncoated polycarbonate Transwell™ filter inserts (3402 Corning Costar Corp., Germany; 3 μm pore size; area, 1.12 cm^2). The medium was changed every day.

Cells were rinsed twice and equilibrated at 37°C for 30 min with pre-warmed assay medium. The assay medium was: 0.4 mM K_2HPO_4, 25.0 mM $NaHCO_3$, 3.0 mM KCl, 1.2 mM $MgSO_4$, 1.4 mM $CaCl_2$, 122.0 mM NaCl, and 10.0 mM glucose. The pH was 7.4 and the osmolarity was 300 mOsm as determined by a freeze point based osmometer (Micro-Osmometer Automatic Type 13 RS, Hermann Roebling Messtechnik, Berlin, Germany). After the assay medium was aspirated, the cells were incubated with 0.5 mL of FITC-NP suspensions for 4 h at particle concentration of 0.25 mg/mL at 37°C. The following FITC-NPs were tested for Confocal Laser Scanning Microscopy (CLSM): FITC-CS NPs, Tween™ 80-coated FITC-CS NPs, FITC-GCS NPs and Tween™ 80-coated FITC-GCS NPs. FITC-CS and FITC-GCS polymers were used as controls. To evaluate efflux mechanisms, VER (0.1 mM) was added in the assay buffer 5 min prior to the addition of NPs at the apical side. After incubation, the test samples were aspirated and the cells were incubated with 0.1 mL of trypan blue for 1 min (0.4% (*w*/*v*) in 0.1 M citrate buffer, pH 4.4), and then, washed away. Trypan blue, by quenching the extracellular fluorescence, enables determination of the fraction of the particles which was actually internalized (28). The cells were washed three times with ice-cold transport buffer, fixated with 3.7% paraformaldehyde in PBS (pH 7.4) for 30 min at room temperature and counter-stained with the cell core marker TO-PRO-3 iodide (134.2 μg/L), for 20 min under light exclusion. Then, chambers were put off the slides and samples were embedded in Gel/Mount™ (Biomeda, Italy), sealed with nail polish and imaged via CLSM (TCS SP2 Leica, Wetzlar, Germany) which was equipped with argon-krypton (488 nm) and helium-neon (633 nm) lasers. The fluorescence was monitored in the following channels: excitation 488 nm (for FITC) and excitation 633 nm (for TO-PRO-3). Slides of untreated cells were used as negative control to determine microscope settings, which were maintained for all image capture and analysis. Confocal images were taken at 500 nm intervals on *z*-axis of the section. Images from individual optical planes and multiple serial optical sections were analyzed and the images were sequentially scanned on the two channels.

Statistics

Data from different experimental groups were compared by a one-way ANOVA with $p<0.05$ at 99% level of confidence (GraphPad Prism v. 4.00 GraphPad Software, Inc. San Diego, CA). Bonferroni post tests were used for post-hoc contrast.

RESULTS

Formation and Characterization of MTX Nanoparticles

Table I shows the physicochemical properties of the different NPs obtained in the presence and in the absence of MTX and/or Tween™ 80. For CS-based NPs, around 250-nm average particle size was found, whereas around 130-nm average particle size was obtained for GCS-based NPs, irrespectively of the presence of MTX and/or Tween™ 80 with the exception of unloaded Tween™ 80 GCS NPs showing average particle size of 210 nm. For all formulations tested, positive zeta values were detected. CS particles exhibited zeta values in the range +30-+23 mV whereas GCS NPs gave zeta values in the range +20-+14 mV. Interestingly, it was noted that Tween™ 80 coating led to a significant lowering of the positive charge.

The A.E. of MTX was also seen to be related to the nature of the polysaccharide employed. Both in the presence and in the absence of Tween™ 80, CS-based nanosystems gave comparable A.E. values close to 30%, whereas GCS NPs and Tween™ 80-coated GCS NPs provided the highest and the lowest association efficiency values of MTX (48% and 19%, respectively).

As for the yield of NP production, MTX-loaded GCS NPs provided the highest yield values (around 50%) while the lowest value was found for unloaded CS-based NPs (18%).

AFM Analysis

AFM was used to investigate the morphology of selected samples (*i.e.*, MTX-loaded GCS NPs- and MTX-loaded Tween™ 80-coated GCS NPs). For each sample the particle size measurements obtained by dynamic light scattering were in good agreement with particle sizes determined by analysis of AFM images. As shown in Fig. 2, most of the particles were spherical with a smooth surface although surrounded by some other material not condensed in the structure of NPs. Our hypothesis is that such material, which was not involved in NP formation, was visualized in the form of aggregates, similarly to the images of unreacted polymer chains as reported by Mao *et al.* (29)

Table I. Physicochemical Properties of Unloaded and MTX-Loaded CS, Tween 80-Coated CS, GCS, and Tween 80-Coated GCS NPs

Formulation	Concentration MTX (% *w*/*v*)	Size (nm)	PI	ζ (mV)	A.E. (%)	Yield (%)
CS NPs	–	245 (±18)	0.31–0.47	+27.1 (±1.6)	–	18 (±1)
MTX-loaded CS NPs	0.05	259 (±27)	0.38–0.47	+30.6 (±1.3)	27 (±8)	37 (±7)
CS Tween80 NPs	–	257 (±45)	0.28–0.40	+23.8 (±0.7)	–	20 (±9)
MTX-loaded CS Tween 80 NPs	0.05	263 (±35)	0.35–0.54	+23.7 (±0.7)	29 (±6)	20 (±5)
GCS NPs	–	132 (±22)	0.14–0.19	+20.0 (±1.7)	–	42 (±8)
MTX-loaded GCS NPs	0.05	140 (±16)	0.11–0.17	+20.1 (±0.8)	48 (±9)	51 (±7)
GCS Tween80 NPs	–	210 (±8)	0.35–0.46	+14.7 (±0.7)	–	20 (±6)
MTX-loaded GCS Tween 80 NPs	0.05	125 (±10)	0.32–0.35	+16.0 (±0.5)	19 (±5)	48 (±8)

PI polydispersity index, ζ zeta potential, *A.E.* association efficiency
Mean±SD are reported ($n=6$)

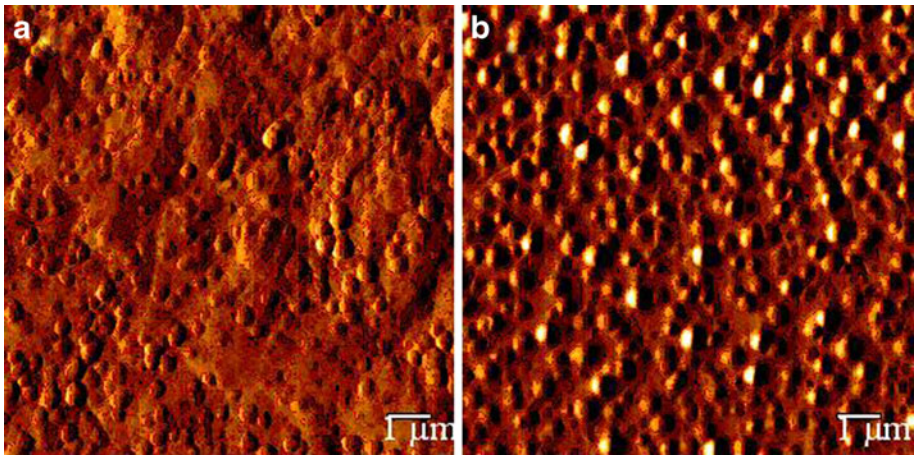

Fig. 2. Atomic force microscopy images of selected MTX NPs. **a** MTX-loaded GCS NPs; **b** MTX-loaded Tween 80-coated GCS NPs

In Vitro Release Study

The results of *in vitro* release tests of NPs are shown in Fig. 3. All NPs studied show a burst phase during the first 6 h and, afterwards, MTX was released from these nanocarriers in a controlled manner until 72 h. Particularly, as shown in Fig. 3, the rank order of drug release rate was: Tween™ 80 GCS NPs>CS NPs>Tween™ 80 CS NPs>GCS NPs.

Cell Viability Studies

In view of transport studies across MDCKII-MDR1, cell viability was assessed according to MTT tests in such cell line using unloaded NPs and the results are reported in Fig. 4. Data show that after 3 h of incubation cells were fully viable (Fig. 4a), irrespectively of the dose and/or the type of particles, but when the assay was prolonged to 24 h, Tween™ 80-coated GCS NPs resulted to give a slight cytotoxic effect (Fig. 4b). On the other hand, MTT tests were also performed in C6 glioma cell line which was proved to be notably more sensitive to the effect of unloaded NPs after 24 h of incubation and the corresponding IC_{50} values are listed in Table II. In this Table, IC_{50} values of MTX-loaded NPs incubated with C6 cell line are also reported and, as shown, GCS-based NPs were the most cytotoxic NPs (IC_{50}=0.04±0.02 µg/mL).

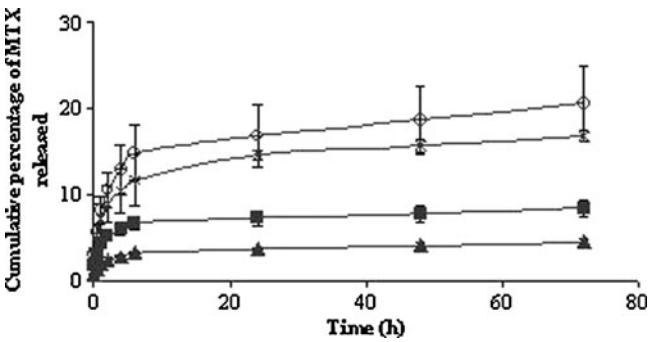

Fig. 3. *In vitro* cumulative release of MTX from NPs in PBS buffer at pH 7.4 in 72 h. Series are: CS NPs (*asterisk*); Tween 80-coated CS NPs (*filled squares*); GCS NPs (*filled up-pointing triangles*); Tween 80-coated GCS NPs (*empty circles*); n=3

Transport Studies in MDCKII-MDR1 Cell Line

The P_{app} values of MTX calculated on the basis of the amounts permeated through MDCKII-MDR1 monolayer during the 3 h of the experiment are given in Table III, together with the enhancement ratio values. P_{app} values determined for NPs were in each case significantly (p<0.01–0.001) greater than pure MTX used as control. The rank order observed in these transport experiments was CS Tween™80 NPs>GCS Tween™ 80 NPs>CS NPs>GCS NPs>>pure MTX.

During the transport experiments, the integrity of the cell monolayer was monitored by recording the TEER (Fig. 5). To gain insight into efflux mechanisms, transport studies were also performed in the presence of VER, a well-

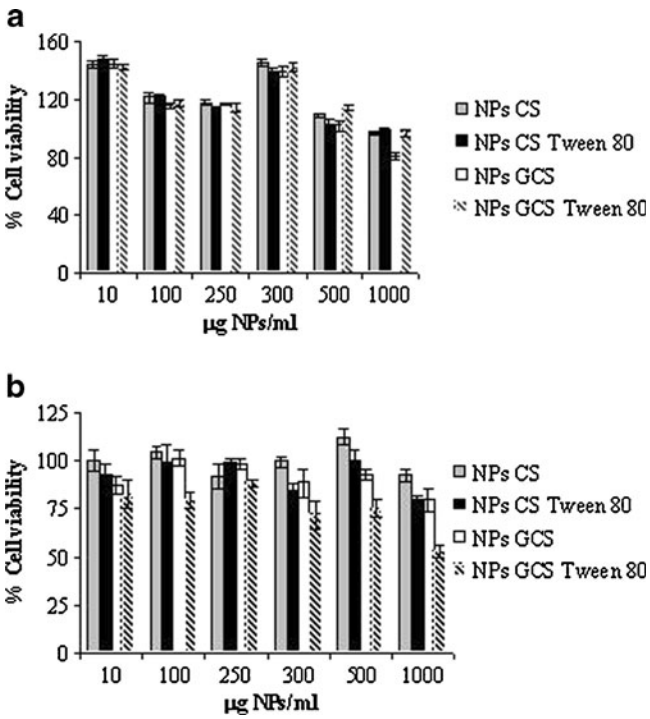

Fig. 4. Cell viability in MDCKII- MDR1 cell line in the presence of unloaded NPs, after incubation of 3 (**a**) and 24 h (**b**). The cell viability was measured *via* the MTT assay. Values represent means±SD (n=8)

Table II. Pure MTX, Unloaded, and MTX-Loaded NPs Induced Cytotoxicity in C6 Cells

	IC_{50} (μg/ml) in C6 cell line
Unloaded NPs CS	414 (±49)*
Unloaded NPs CS Tween 80	766 (±37)*
Unloaded NPs GCS	141 (±1)*
Unloaded NPs GCS Tween 80	80 (±37)*
MTX-loaded NPs CS	0.11 (±0.02)*
MTX NPs-loaded CS Tween 80	0.08 (±0.009)*
MTX-loaded NPs GCS	0.04 (±0.02)*
MTX-loaded NPs GCS Tween 80	0.09 (±0.002)*
Pure MTX	0.0009 (±0.0005)

The cells were treated with pure MTX, unloaded NPs, and MTX-loaded NPs for 24 h. The cell viability was measured via the MTT assay and compared to a control (*i.e.*, pure MTX). Values represent means±SD (n=8)
*p<0.001, significantly different from MTX control

known P-gp inhibitor. Without VER pre-treatment, no significant TEER% decrease was detected for GCS and Tween™ 80 GCS NPs (Fig. 5), and it supports the conclusion that the monolayer maintains its integrity during these experiments. In contrast, by using CS and Tween™ 80 CS NPs an apparent decrease of TEER up to 3 h of permeation was measured and an almost complete recovery of the initial TEER values was observed after 24 h. In the permeation experiments, FD4 and DZ were also used as markers of paracellular and transcellular transport, respectively. According to the data reported in Table IV, for both GCS NPs and Tween™ 80-coated GCS NPs, the permeation of MTX does not proceed through paracellular pathway as confirmed by the finding that the P_{app} of FD4 did not significantly change with respect to the control value ($0.23\ 10^{-6}$±$0.04\ 10^{-6}$ and $0.25\ 10^{-6}$±$0.03\ 10^{-6}$ cm/s for GCS NPs and Tween™ 80-coated GCS NPs, respectively). Moreover, all tested NPs provided DZ P_{app} values similar to the control.

Confocal Microscopy in MDCKII-MDR1 Cell Line

The uptake of FITC-NPs across MDCKII-MDR1 was studied by CLSM in the presence and in the absence of VER. TO-PRO 3 was used as a marker for MDCKII-MDR1 cell nuclei giving a typical blue fluorescence (30) and to distinguish between membrane-associated and internalized complexes, Trypan blue was employed throughout the study. It is

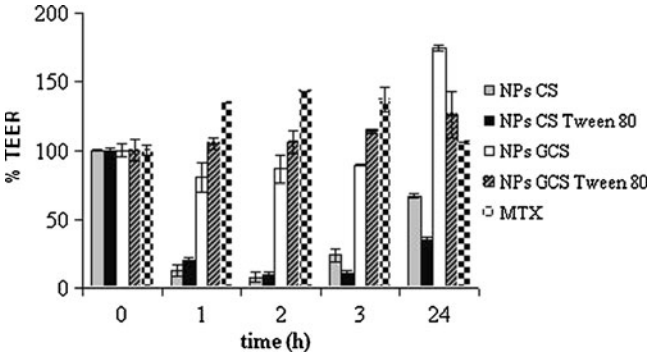

Fig. 5. TEER% variations during the MTX NPs permeation test across MDCKII-MDR1 cells. No VER pre-treatment of the cells was carried out. Data are mean±SD (n=6)

well known that viable cells exclude Trypan blue molecules; consequently, the residual fluorescence implied the existence of a substantial amount of intracellular NPs, rather than cell surface adsorption. On the membranes of the cells subjected to VER pre-treatment (Fig. 6e–h), brilliant green fluorescent NPs were observed and, additionally, the labeled carriers were detected with a stronger fluorescence intensity than that without VER pre-treatment. Reasonably, VER is responsible of change in membrane fluidity and allows a higher accumulation of the fluorescent particles around cell membranes (31). In our cases, almost none of fluorescent GCS NPs were detected after incubation with the cells without any VER pre-treatment (Fig. 6c), but the same particles were revealed as *loci* of green fluorescence when the cells were previously treated with VER (Fig. 6g).

DISCUSSION

The main aim of the present study was to compare the *in vitro* performance of CS- and GCS-based NPs coated with Tween™ 80 for the administration of MTX to brain tumors where the BBB consists of both a leaky moiety and an intact and functional part. For this purpose, CS- and GCS-based NPs were prepared following a modified procedure of the ionic gelation technique (22). MTX is insoluble in water and ethanol whereas it dissolves in dilute solutions of alkaline hydroxides and carbonates. Therefore, the drug was dissolved in the basic solution of TPP (pH 9) before crosslinking CS (or GCS) alone or in the presence of Tween™ 80. In this work, the concentration of the coating surfactant was selected equal to 0.1% (v/v), 10 and 20 times lower than that used by

Table III. P_{app} of MTX Permeated Alone and from Tested NPs After 3 h Through MDCKII-MDR1 Cells

	P (cm/s 10^{-6}) MTX (without VER)	Enhancement ratio (%; without VER)	P (cm/s 10^{-6}) MTX (with VER)	Enhancement ratio (%; with VER)
MTX	0.60 (±0.03)	–	0.52 (±0.02)	–
CS NPs	24.31 (±2.47)**	40.52	30.14 (±6.51)**	57.96
CS Tween 80 NPs	36.83 (±17.58)**	61.38	48.71 (±24.01)**	93.67
GCS NPs	19.29 (±9.76)*	32.15	23.41 (±6.82)*	45.02
GCS Tween 80 NPs	29.60 (±5.36)**	49.33	40.82 (±13.09)**	78.50

Cells were not pre-treated with VER (without VER; columns 1 and 2). Cells were pre-treated with VER (with VER; columns 3 and 4). Data are mean±SD (n=8)
*p<0.01 *versus* control MTX; **p<0.001 *versus* control MTX

Table IV. P_{app} Values of FD4 and DZ Permeated After 3 h Across MDCKII-MDR1 Cells

Treatment	P_{app} FD4 ($\times 10^{-6}$ cm/s)	P_{app} DZ ($\times 10^{-6}$ cm/s)
MTX	0.18±0.001*	13.46±0.10**
CS NPs	1.25±0.05**	5.94±0.67
CS Tween 80 NPs	1.84±0.06**	5.78±0.81
GCS NPs	0.23±0.04	3.92±0.45
GCS Tween 80 NPs	0.25±0.03	3.38±0.51
FD4	0.26±0.04	–
DZ	–	3.09±2.17

No VER pre-treatment of the cells was applied. Data are mean±SD (n=6)
*p<0.05 *versus* control FD4 (or DZ); **p<0.001 *versus* control FD4 (or DZ)

Kreuter for poly(butylcyanoacrylate) NPs (5) and Soni *et al.* in the case of CS NPs (20), respectively. Our objective was to investigate if at relatively low concentration of Tween™ 80—with minimized side effects caused by the surfactant—still allows the particles to cross the BBB. In addition, in preliminary experiments, it was noted that, by working at a final concentration of the surfactant equal to 1% v/v, particle size distribution resulted bigger than 0.4 and the presence of marked foam made difficult the work-up (data not shown). Furthermore, instead of coating the particles after their formation as described in Soni *et al.* (20), herein, we attempted to achieve the physical coating by mixing CS (or GCS) solutions with Tween™ 80 under constant magnetic stirring at room temperature, before the addition of TPP containing MTX solution. As a result of this preparation method, it can be expected a uniform mixture of Tween™ 80 and polymer so that the final NPs surface should be made up of polymer and Tween™ 80. In particular, our Tween™ 80 coated NPs should be intended, indeed, as particles coated by a hybrid mixture of surfactant and polymer rather than completely coated with Tween™ 80.

As shown in Table I, CS NPs were found bigger in size than the corresponding GCS NPs due to the higher average molecular weight of the former polymer, even though several factors cannot be ruled out among which the concentration of the polysaccharide, the concentration of TPP and the ratio polycation/polyanion (32). Concerning zeta potential values, again, the molecular weight of the polymer affected the measured values (33) and the decrease of zeta potential for Tween™ 80-coated NPs values confirmed the hypothesis that at least some of the surfactant is located on the outer surface of the particles.

For all types of particles, MTX entrapment can be mainly explained in terms of electrostatic interactions occurring between the carboxylate group of the drug with the positive charges of the polymer. To account for the highest MTX A.E. value of GCS NPs, not only the above mentioned interactions should be considered, but also hydrogen bonding interactions between the –OH pendant groups of GCS and the polar groups of MTX could be involved. Probably, the latter interactions are diminished when Tween™ 80 covers GCS NPs, so leading to a reduced A.E. (*i.e.*, 19%).

From the analysis of release profiles (Fig. 3), the initial burst phase can be related to the drug adsorbed onto the external surface of the particles that rapidly comes out whereas MTX deeply entrapped inside the matrices of CS and GCS is then released in a controlled manner, reaching about 20% in the case of GCS NPs after 72 h. Thus, all NPs seem to act as MTX reservoirs allowing a slow release of MTX in the tumor area, once the BBB is crossed. Such slow

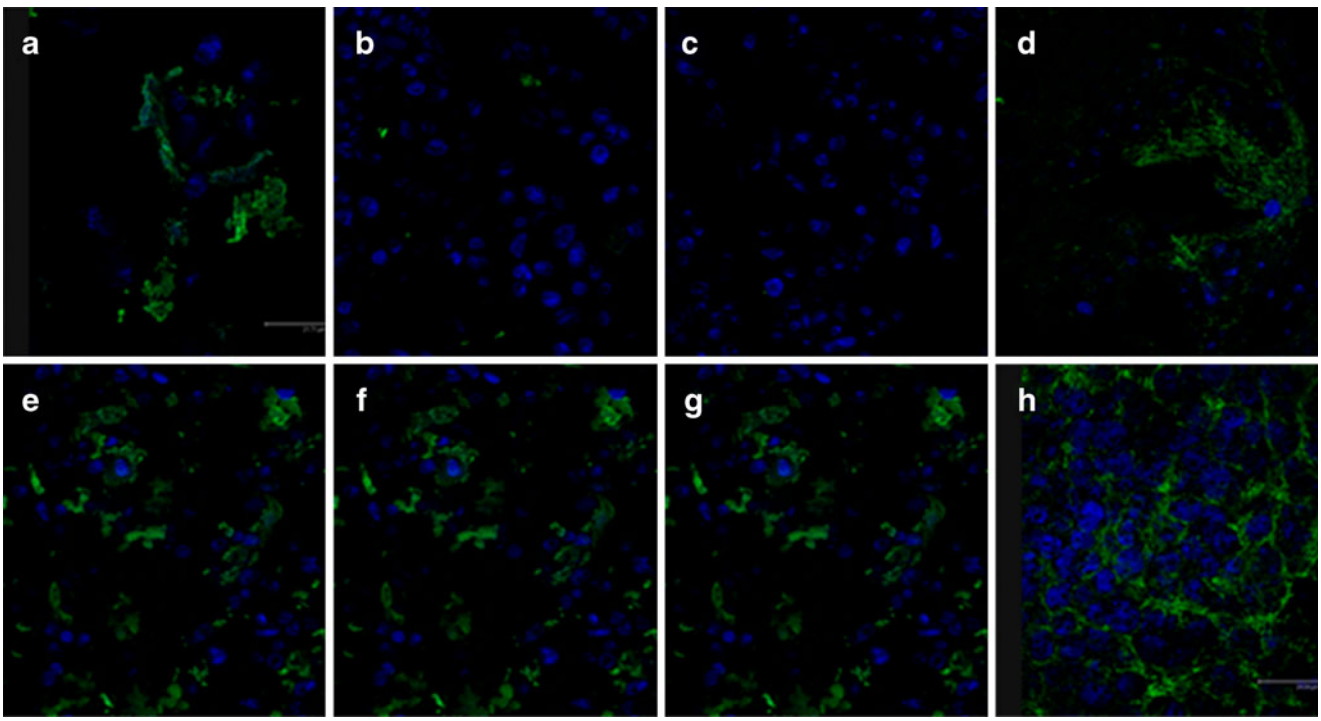

Fig. 6. *In vitro* confocal images of different unloaded FITC-labeled NPs incubated in MDCKII-MDR1 monolayer for 4 h at 37°C. **a** CS NPs; **b** Tween 80-coated CS NPs; **c** GCS NPs; **d** Tween 80-coated GCS NPs. From (**e**–**h**), the cells were pre-treated with VER for 5 min: **e** CS NPs; **f** Tween 80-coated CS NPs; **g** GCS NPs; **h** Tween 80-coated GCS NPs. Confocal images were taken at 500-nm intervals on z-axis of the section

release profile could be related to the fact that swellable polymers such as CS and GCS (alone or in the presence of Tween™ 80) arrange themselves to constitute a gel-like barrier limiting the diffusion of the drug into the medium.

The cytotoxic effect of the unloaded and MTX-loaded NPs was evaluated in the presence of two cell lines: MDCKII-MDR1 and C6 glioma cell lines. MDCKII-MDR1 are cells originating from dog renal distal tubular epithelium transfected with the human MDR1 gene encoding for P-gp and are recommended as a model of *in vitro* human BBB (21). MDCKII-MDR1 cells overexpress the efflux pump P-gp and exhibit a quite high transepithelial electrical resistance (34). For MDCKII-MDR1 cell line, cells were found essentially viable. Glioma C6 cell line is herein adopted as an *in vitro* prototype of brain tumor. From MTT test in C6 cell line, as expected, MTX containing NPs were found around 90–360-fold less cytotoxic than the pure drug. Overall, to explain the cytotoxicity of the tested cells to both unloaded and MTX-loaded particles, the high number of positive charges in CS and GCS polycations should be invoked in the interactions with the negatively charged cell membranes components (*i.e.*, sialic acids) as also suggested by Hu and coworkers (35). Data also show that GCS-based NPs seem to be more toxic than CS based NPs, probably because the former are smaller than the latter and, consequently, the positive charge density is enhanced in the former case. Moreover, it should be noted that when MTX is delivered from the NPs, it causes the toxic build up of cellular intermediates of the folic acid cycle, so reducing cellular viability and, ultimately, causing cellular mortality (36).

In vitro BBB penetration studies revealed that, although not statistically significant, the coating with the surfactant Tween™ 80 brought about a clear positive effect on the drug permeability (compare the P_{app} values of CS NPs with CS Tween™ 80 NPs and of GCS NPs with GCS Tween™ 80 NPs). Such effect is similar to that observed not only for Tween™ 80 coated polybutylcyanoacrylate NPs (5) but also for CS NPs by Soni and coworkers (20). On the other hand, Tween™ 80 is able to inhibit P-gp as shown by Friche *et al.* (37), and it may increase the permeation of the unencapsulated MTX released from NPs at level of the intact barrier. It was confirmed from the transport studies results that, when VER pre-treatment of the cells was carried out, (Table III) for each type of particles, the P_{app} values were found in the same rank order, but numerically increased. It is noteworthy that the enhancement ratios were up to 93.67 and 78.50% for CS Tween™ 80 NPs and GCS Tween™ 80 NPs, respectively.

From a mechanism viewpoint, we assume that the transport of the CS- and GCS-based NPs across the MDCKII-MDR1 monolayer occurs as follows. Where the BBB is disrupted, our NPs can be taken up by EPR effect, whereas across the intact BBB an adsorbitive-mediated transcytosis (AMT) takes place. AMT is a transport mechanism dependent on the electrostatic interaction between the positively charged NPs and the negatively charged membrane of the monolayer (38). Due to its high molecular weight and hydrophilic character, FD4 is a fluorescent probe which can only permeate through the MDCKII-MDR1 monolayer when the tight junctions are opened and, hence, constitutes a marker of the paracellular transport mechanism. For both CS and Tween™ 80 CS NPs, along with an AMT transport, the opening of tight junctions of MDCKII-MDR1 monolayer operated by NPs could occur as confirmed by the increase of FD4 P_{app} value (Table IV). In fact, the strong TEER% decrease combined with the increasing of P_{app} of FD4 are the two main evidences of the paracellular permeation of MTX. The behavior of CS and Tween™ 80 CS NPs could be explained in terms of the well-known capability of chitosan polymer at high deacetylation degree (>85%) (39) to enhance the paracellular passage through tight junctions (40). On the other hand, the P_{app} values of DZ for NPs were comparable with DZ taken as control, suggesting that the particles do not permeate through the transcellular pathway.

To gain insight on the uptake of the NPs, the polymers CS and GCS were previously FITC labeled to be detected under the confocal microscope. The CLSM images referring to Tween™ 80-coated GCS NPs (Fig. 6d, h) indicating that not only the surfactant may facilitate the BBB penetration, enhancing the distribution of the particles in the whole monolayer, but also the small size could be favorable for internalization. On the other hand, CLSM microphotographs in Fig. 6e, f indicate that NP transport across the cells was enhanced by the selective blockage of the efflux pump (*i.e.*, under VER pre-treatment), supporting a paracellular pathway for CS and between 80 CS NPs.

CONCLUSIONS

In this study, NPs made of CS and GCS (with and without Tween™ 80-coating layer) have been successfully formulated as delivery systems for the anticancer drug MTX. Transport experiments across MDCKII-MDR1 show that even a relatively low concentration of Tween™ 80 used in NPs coating (0.1%, *v*/*v*) allows the overcoming of the BBB. Moreover, drug loaded NPs displayed cytotoxic effects against C6 glioma cell line taken as a model brain tumor. Importantly, MTX-loaded GCS NPs seem slightly more cytotoxic than CS-based ones. Therefore, these nanocarriers represent a promising strategy for the administration of the antineoplastic MTX to brain tumor which merits further investigations under *in vivo* conditions. Further studies will be addressed to *in vivo* administration of the reported particles.

ACKNOWLEDGMENTS

This project was financed by Università degli Studi di Bari (Progetti di Ateneo 2008). We thank Dr. Antonella Loverre (Dipartimento di Emergenza Trapianti di Organi, (D.E.T.O.) Bari Hospital, Bari, Italy) for interpretation of confocal microphotographs. We also thank Prof. Giuseppe Trapani (University of Bari) for helpful discussions.

Declaration of interest statement The authors state no conflict of interest.

REFERENCES

1. Blakeley J. Drug delivery to brain tumors. Curr Neur Neurosci Rep. 2008;8:235–41.
2. Laquintana V, Trapani A, Denora N, Wang F, Gallo JM, Trapani G. New strategies to deliver anticancer drugs to the Central Nervous System. Expert Opin Drug Deliv. 2009;6:1017–32.

3. Provenzale JM, Mukundan S, Dewhirst M. The role of blood-brain barrier permeability in brain tumor imaging and therapeutics. Am J Roentgenol. 2005;185:763–7.
4. Tosi G, Costantino L, Ruozi B, Forni F, Vandelli MA. Polymeric nanoparticles for the drug delivery to the central nervous system. Exp Opin Drug Deliv. 2008;5:155–74.
5. Kreuter J, Ramge P, Petrov V, Hamm S, Gelperina SE, Engelhardt B, *et al*. Direct evidence that polysorbate-80-coated poly(butylcyanoacrilate) nanoparticles deliver drugs to the CNS via specific mechanisms requiring prior binding of drug to the nanoparticles. Pharm Res. 2003;20:409–16.
6. Gelperina S, Maksimenko O, Khalansky A, Vanchugova L, Shipulo E, Abbasova K, *et al*. Drug delivery to the brain using surfactant-coated poly(lactide-co-glycolide) nanoparticles: influence of the formulation parameters. Eur J Pharm Biopharm. 2010;74:157–63.
7. Zensi A, Begley D, Pontikis C, Legros C, Mihoreanu L, Wagner S, *et al*. Albumin nanoparticles targeted with Apo E enter the CNS by transcytosis and are delivered to neurones. J Control Release. 2009;137:78–86.
8. Morris PG, Abrey LE. Therapeutic challenges in primary CNS lymphoma. Lancet. 2009;8:581–92.
9. Duthie SJ. Folic acid-mediated inhibition of human colon cancer cell growth. Nutrition. 2001;17:736–7.
10. Kuznetsova N, Kandyba A, Vostrov I, Kadykov V, Gaenko G, Molotkovsky J, *et al*. Liposomes loaded with lipophilic prodrugs of methotrexate and melphalan as convenient drug delivery vehicles. J Drug Del Sci Tech. 2009;19:51–9.
11. Dhanikula RS, Argaw A, Bouchard JF, Hildgen P. Methotrexate loaded polyether-copolyester dendrimers for the treatment of gliomas: enhanced efficacy and intratumoral transport capability. Mol Pharm. 2008;5:105–16.
12. Denora N, Trapani A, Laquintana V, Lopedota A, Trapani G. Recent advances in medicinal chemistry and pharmaceutical technology-strategies for drug delivery to the brain. Curr Top Med Chem. 2009;9:182–96.
13. Csaba N, Garcia-Fuentes M, Alonso MJ. The performance of nanocarriers for transmucosal drug delivery. Expert Opin Drug Del. 2006;3:463–78.
14. Trapani A, Lopedota A, Franco M, Cioffi N, Ieva E, Garcia-Fuentes M, *et al*. A comparative study of chitosan and chitosan/cyclodextrin nanoparticles as potential carriers for the oral delivery of small peptides. Eur J Pharm Biopharm. 2010;75:26–32.
15. Ieva E, Trapani A, Cioffi N, Ditaranto N, Monopoli A, Sabbatini L. Analytical characterization of chitosan nanoparticles for peptide drug delivery applications. Anal Bioanal Chem. 2009;393:207–15.
16. Du Y, Ding Y, Sun M, Zhang L, Jiang X, Yang C. Hollow chitosan/poly(acrylic acid) nanospheres as drug carriers. Biomacromolecules. 2007;8:1069–76.
17. Son YJ, Jang J-S, Cho YW, Chung H, Park R-W, Kwon I-C, *et al*. Biodistribution and anti-tumor efficacy of doxorubicin loaded glycol-chitosan nanoaggregates by EPR effect. J Control Release. 2003;91:135–45.
18. Hwang HY, Kim I-S, Kwon IC, Kim YH. Tumor targetability and antitumor effect of docetaxel-loaded hydrophobically modified glycol chitosan nanoparticles. J Control Release. 2008;128:23–31.
19. Min KH, Park K, Kim Y-S, Bae SM, Lee S, Jo HG, *et al*. Hydrophobically modified glycol chitosan nanoparticles-encapsulated camptothecin enhance the drug stability and tumor targeting in cancer therapy. J Control Release. 2008;127:208–18.
20. Soni S, Babbar AK, Sharma RK, Banerjee T, Maitra A. Pharmacoscintigraphic evaluation of polysorbate80-coated chitosan nanoparticles for brain targeting. Am J Drug Del. 2005;3:205–12.
21. Mensch J, Oyarzabal J, Mackie C, Augustijns P. *In vivo*, *in vitro* and *in silico* methods for small molecule transfer across BBB. J Pharm Sci. 2009;98:4429–68.
22. Trapani A, Sitterberg J, Bakowsky U, Kissel T. The potential of glycol chitosan nanoparticles as carrier for low water soluble drugs. Int J Pharm. 2009;375:97–106.
23. Lopedota A, Trapani A, Cutrignelli A, Chiarantini L, Pantucci E, Curci R, *et al*. The use of Eudragit RS 100/cyclodextrin nanoparticles for the transmucosal administration of glutathione. Eur J Pharm Biopharm. 2009;72:509–20.
24. Gaillard PJ, de Boer AG. Relationship between permeability status of the blood-brain barrier and *in vitro* permeability coefficient of a drug. Eur J Pharm Sci. 2000;12:95–102.
25. Park J, Han TH, Lee KY, Han SS, Hwang JJ, Moon DH, *et al*. N-acetyl histidine-conjugated glycol chitosan self assembled nanoparticles for intracytoplasmic delivery of drugs: endocytosis, exocytosis and drug release. J Control Release. 2006;115:37–45.
26. de Campos A, Diebold Y, Carvalho ELS, Sanchez A, Alonso MJ. Chitosan nanoparticles as new ocular drug delivery systems: *in vitro* stability, *in vivo* fate, and cellular toxicity. Pharm Res. 2004;21:803–10.
27. Huang M, Ma Z, Khor E, Lim LY. Uptake of FITC-chitosan nanoparticles by A549 cells. Pharm Res. 2002;19:1488–94.
28. Behrens I, Vila Pena AI, Alonso MJ, Kissel T. Comparative uptake studies of bioadhesive and non-bioadhesive nanoparticles in human intestinal cell lines and rats: the effect of mucus on particle uptake adsorption and transport. Pharm Res. 2002;19:1185–93.
29. Mao S, Bakowsky U, Jintapattanakit A, Kissel T. Self assembled polyelectrolyte nanocomplexes between chitosan derivatives and insulin. J Pharm Sci. 2006;95:1035–48.
30. Loverre A, Ditonno P, Crovace A, Gesualdo L, Ranieri E, Pontrelli P, *et al*. Ischemia-reperfusion induces glomerular and tubular activation of proinflammatory and antiapoptotic pathways: differential modulation by rapamycin. J Am Soc Nephrol. 2004;15:2675–86.
31. Kamau SW, Kramer SD, Gunthert M, Wounderlj-Allenspach H. Effect of the modulation of the membrane lipid composition on the localization and function of P-glycoprotein in MDR1-MDCK cells. *In vitro* Cell. Dev Biol Anim. 2005;41:207–16.
32. Janes KA, Calvo P, Alonso M. Polysaccharide colloidal nanoparticles as delivery systems for macromolecules. Adv Drug Del Rev. 2001;47:83–97.
33. Gan Q, Wang T, Cochrane C, McCarron P. Modulation of surface charge, particle size and morphological properties of chitosan–TPP nanoparticles intended for gene delivery. Colloids Surf B Biointerfaces. 2005;44:65–73.
34. Wang Q, Rager JD, Weinstein K, Kardos PS, Dobson GL, Li J, *et al*. Evaluation of the MDR-MDCK cell line as permeability screen for the blood–brain barrier. Int J Pharm. 2005;288:349–59.
35. Hu Y, Ding Y, Ding D, Sun M, Zhang L, Jiang X, *et al*. Hollow chitosan/poly(acrylic acid) nanospheres as drug carriers. Biomacromolecules. 2007;8:1069–76.
36. Kohler N, Sun C, Wang J, Zhang M. Methotrexate-modified superparamagnetic nanoparticles and their intracellular uptake into human cancer cells. Langmuir. 2005;21:8558–64.
37. Friche E, Jensen PB, Sehested M, Demant EJ, Nissen NN. The solvents Cremophor EL and between 80 modulate daunorubicin resistance in the multidrug resistant Ehrlich ascites tumor. Cancer Commun. 1990;2:297–303.
38. Beduneau A, Saulnier P, Benoit J-P. Active targeting of brain tumors using nanocarriers. Biomaterials. 2007;28:4947–67.
39. Janes KA, Alonso MJ. Depolymerized chitosan nanoparticles for protein delivery: preparation and characterization. J Appl Polym Sci. 2003;88:2769–76.
40. Bonferoni MC, Sandri G, Rossi S, Ferrari F, Gibin S, Caramella C. Chitosan citrate as multifunctional polymer for vaginal delivery. Evaluation of penetration enhancement and peptidase inhibition properties. Eur J Pharm Sci. 2008;33:166–76.